

Ab initio cluster study of the interaction of fluorine and chlorine with the Si(111) surface

M. Seel* and P. S. Bagus

IBM Research Laboratory, San Jose, California 95193

(Received 4 February 1983)

The interaction of atomic fluorine and chlorine with the Si(111) surface has been studied by using clusters of Si atoms to simulate the substrate. The largest cluster contains ten Si atoms, representing the first four layers of the Si surface. An F or Cl atom is added to three high-symmetry adsorption sites. In the on-top site, the halogen adatom is directly above a surface Si atom. The open and eclipsed sites are both threefold with the adatom at the center of a triangle of first-layer atoms. In the open site, the adatom is directly above a fourth-layer Si while in the eclipsed site it is above a second-layer Si. *Ab initio* Hartree-Fock wave functions have been calculated, and the energy of the system is studied as a function of the vertical distance of the adatom from the surface (first) Si layer. Equilibrium bond distances, vibrational energies of the adatoms, and binding energies for adsorption are calculated. Bonding mechanisms and properties for the different sites are compared. For the on-top site, the binding energy D_e is 3.2 eV (1.6 eV) for F (Cl), and the equilibrium distance from the surface r_e is 1.7 Å (2.2 Å). For F at the open site, two attractive minima are found: $R_e = 1.3$ and -1.4 Å; D_e is found to be ~ 0.5 eV for both positions, the barrier height for penetration is ~ 1 eV. For Cl at this open site, D_e is 0.4 eV and r_e is 1.9 Å. The barrier height is 13 eV. At the eclipsed site, D_e is 0.5 eV (0.2 eV) for F (Cl) with r_e being 1.7 Å (2.2 Å). The calculated D_e 's for Cl indicate that the most stable chemisorption site for Cl on Si(111) is the onefold on-top site. The vibrational energies for the motion of Cl normal to the surface are found to be substantially different for sites with different surface coordination and should be experimentally accessible in electron-energy-loss spectroscopy. The difference of calculated core-ionization energies for F at the on-top site and at the open site are compared with observed x-ray photoelectron spectroscopy data. This comparison suggests the formation of an intermediate-surface species, where the F atom has penetrated into the lattice, before the final product, volatile SiF₄, of the reaction between F and Si is formed. All the results are in agreement with the observed different reactivity of F and Cl with Si. They provide a model for understanding reactions relevant in plasma etching.

I. INTRODUCTION

Adsorption processes and chemical reactions on semiconductor surfaces have been extensively investigated in the past few years both theoretically and experimentally.¹ Silicon, with and without chemisorbed overlayers, is probably the most studied surface. The interaction of F and Cl and Si has become of particular interest because of the role of halogen-containing radicals in plasma etching of Si and Si-compound surfaces.²⁻⁴ Plasma etching is playing an increasingly important role in the manufacture of semiconductor devices. F and Cl radicals show different reactivity at a Si surface, either a polycrystalline film^{3,5} or a single crystal.^{6,7} Fluorine radicals, arising at the surface, for example, from the dissociative adsorption of XeF₂, react spontaneously to form volatile species, predominantly SiF₄, at a rapid rate.^{5,6} However, Cl radicals arising at the surface from the dissociative adsorption of Cl₂ do not react spontaneously at any appreciable rate under normal conditions.³ Instead, on Si(111) they form an ordered overlayer being chemisorbed, almost certainly, at directly overhead sites.⁷ Yet both SiF₄ and SiCl₄ are volatile species and the reactions to form these molecules at a Si surface are very exothermic: That to form SiF₄ from the dissociation of XeF₂ is exothermic by 397 kcal/mole = 17.2 eV (Refs. 8 and 9) and that to form SiCl₄ from Cl₂ by

$$157 \text{ kcal/mole} = 6.8 \text{ eV.}^8$$

The chemisorption of Cl on Si(111) has been also widely studied. Comparison of polarized or angle-resolved photoemission data with tight-binding band-structure-type calculations strongly suggests the onefold site for chemisorbed Cl atoms^{7,10-13} (a single chlorine atom sits on top of a surface Si atom). For fluorine there exists only one non-self-consistent slab calculation¹⁴ where a two-dimensional periodic F adsorbate layer is considered with F at both onefold and threefold chemisorption sites. However, there are no experimental data available to compare with these results. Only recently, evidence was found for the formation of intermediate-surface species in this reaction.¹⁵

The main objective of this study is to help to understand and explain the different reactivities of atomic fluorine and chlorine with the silicon surface. Of the different theoretical approaches¹⁶ for the quantitative description of the interaction between adatoms (or molecules) and a solid surface, the cluster model is used for this study. In this approach a small number of atoms representing the surface plus a chemisorbed atom or molecule are considered as a quasimolecule. Wave functions are determined for this quasimolecule and its properties interpreted in terms of processes on an extended surface. One obtains a detailed picture of the modification of the

individual orbitals of the adatom by the presence of the surface atoms (and, of course, vice versa). The principal properties of interest, such as equilibrium geometry on the surface, the vibrational energies of the adatom, binding energy for adsorption, and shifts between photoemission spectra of free and chemisorbed atoms or molecules, can be calculated. Self-consistent-field (SCF) Hartree-Fock (HF) calculations for different adatom-substrate systems, such as H-Be,¹⁷ H-Si,¹⁸ O-Li,¹⁹ CO, and N₂-Ni,²⁰ and the comparison of their results with experimental data demonstrate the accuracy and suitability of the cluster-model approach.

We study the interaction of atomic fluorine and chlorine with the Si(111) surface at three high-symmetry sites: on top, open, and eclipsed. The *ab initio* Hartree-Fock linear combination of atomic orbitals (LCAO) method is used to calculate the electronic structure of different silicon clusters with an F or Cl atom added at these three sites. The adatom-substrate energy is studied as a function of vertical distance of the adatom from the surface. Equilibrium bond distances, vibrational energies of the adatoms, and binding energies for adsorption are calculated. The comparison of the bonding mechanisms and properties for the different sites shows characteristic differences in the adsorption parameters for the three sites and for the two halogens. Specifically, the results corroborate that the most stable chemisorption site for Cl on Si(111) is the onefold on-top site. It is further shown that at the open site, fluorine atoms can penetrate into the Si lattice by going over a relatively small barrier. By contrast, the barrier for Cl penetration is very high. The comparison with experiment¹⁵ of calculated core-ionization energies for F above the surface at the on-top site and below the surface at the open site suggests the formation of intermediate-surface species during the reaction of fluorine with the Si surface. The results for the vibrational energies for Cl chemisorbed at sites with different surface coordination are sufficiently different to suggest the value of electron-energy-loss spectroscopy (EELS) experiments as an additional test for the chemisorption site of Cl on Si and to further test the cluster-model calculation.

This paper is organized as follows. In Sec. II we discuss the computational details of our calculations. The cluster models are described in Sec. II A, Sec. II B presents the details of the electronic structure calculations, and Sec. II C introduces the choice and optimization of basis sets and symmetry considerations. In Sec. III we present the results for the silicon-substrate clusters; Sec. III A gives the results for the clusters used to model the on-top site, Sec. III B presents results for the open site, and Sec. III C gives results for the eclipsed site. In Sec. IV the Si-F data are presented; in Secs. IV A–IV C we discuss the results for the three different fluorine adsorption sites; in Sec. IV D the F core-ionization energies are compared with the observed x-ray photoemission spectroscopy (XPS) data.¹⁵ The Si-Cl results are discussed in Sec. V. Sections V A–V C contain the data for the three different chlorine adsorption sites. In Sec. V D we analyze the vibrational frequencies in terms of a simple spring model. Finally in Sec. VI we compare the F and Cl results and give our conclusions for the interaction of these two halogens with the Si(111) surface.

II. COMPUTATIONAL DETAILS

A. Cluster models for the high-symmetry sites at the Si(111) surface

As is the case for many surfaces, Si(111) relaxes and reconstructs; i.e., the positions of the surface atoms in the first few layers of the crystal change from their positions in the bulk.²¹ In the cluster models used for the present study, these changes are neglected and the Si atoms are chosen to have their bulk geometry,²² $d_{\text{Si-Si}} = 4.44$ bohrs. (There is evidence that the displacements of the surface Si atoms on Si(111) are reasonably small.²³) On this ideal Si(111) surface, each surface Si atom has three nearest neighbors in the second layer, as shown in Fig. 1, rather than the four nearest neighbors for a tetrahedrally coordinated bulk atom. Assuming sp^3 hybridization as in the bulk, each surface atom has one unpaired electron, the dangling bond, which has essentially sp_z character.

When an adatom stabilizes directly above a silicon atom of the first layer, we call this position the onefold, head-on, or on-top adsorption site. To model this situation we consider two halogen-silicon clusters of different size. The smallest substrate cluster contains four Si atoms: one on the surface (first layer) and its three nearest neighbors in the second layer, 1.48 bohrs below the surface. In order to stimulate the remainder of the crystal, the same embedding procedure as for the H-Si(111) study¹⁸ is applied: Each edge Si atom of the second layer is given three hydrogen-atom neighbors placed at the Si-H distance in SiH₄, $d_{\text{Si-H}} = 2.80$ bohrs. This ensures that every Si atom in the cluster has its proper atomic coordination: three for the surface Si and four, one Si and three H atoms, for the second-layer Si. The hydrogen atoms force the second-layer Si atoms to have the bulk sp^3 hybridization and effectively saturate the edges of the cluster. [For a covalently bonded semiconductor such as Si, this is most likely a satisfactory procedure. Its use is supported by the results of the H-Si(111) study.¹⁸] The total composition of this cluster is Si₄H₉ [see Fig. 2(a)]. The interaction at this site is studied by adding an X ($X = \text{F, Cl}$) atom above the surface Si.

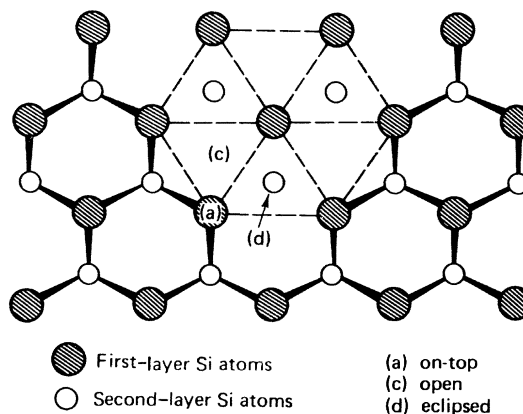


FIG. 1. Schematic of the Si(111) surface showing first- and second-layer Si atoms. The two kinds of threefold sites, open and eclipsed, are indicated by dashed lines. Representative on-top, open, and eclipsed sites are labeled with letters *a*, *c*, and *d*.

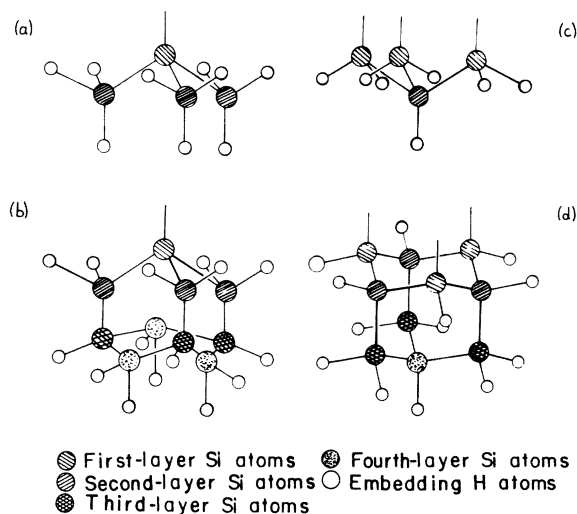


FIG. 2. (a) The two-layer Si_4H_7 cluster used to model the on-top site of $\text{Si}(111)$; (b) the four-layer $\text{Si}_{10}\text{H}_{15}$ cluster used to model the on-top site; (c) the two-layer Si_4H_7 cluster used to model the eclipsed site; (d) the four-layer $\text{Si}_{10}\text{H}_{13}$ cluster used to model the open site of $\text{Si}(111)$. The dangling bonds of the first-layer Si atoms are indicated.

In the second cluster we include three Si atoms each in the third (5.92 bohrs below the surface) and fourth layer (7.40 bohrs below the surface). As before, embedding H atoms are used to form a tetrahedral bulk environment for the Si atoms and to effectively allow for sp^3 hybridization. The second-layer Si atoms each have two H neighbors; the third-layer Si atoms have one H, the fourth-layer Si atoms have two H neighbors. This $\text{Si}_{10}\text{H}_{15}$ cluster is shown in Fig. 2(b). By studying the properties of these two clusters of different size we can learn about the convergence of different adsorption properties with respect to cluster size, an important problem for the cluster-model approach.^{17(b)}

Consider now the threefold equilateral triangle, sites on $\text{Si}(111)$ shown by dashed lines in Fig. 1. Each surface atom is surrounded by six of these sites. For three of the sites there is a second-layer Si atom in the center of the triangle; these sites are called eclipsed sites. For the other three sites, the first Si atom below is in the fourth layer (7.40 bohrs \approx 3.9 Å below the surface); these open sites are, on $\text{Si}(111)$, the most likely sites at which an atom could penetrate the surface. The interaction at these sites is studied by adding the halogen atom along a line normal to the center of the equilateral triangle.

The surface cluster chosen to model the eclipsed site contains four Si atoms and seven embedding H atoms, Si_4H_7 . Three Si atoms are in the first layer (surface) and one is in the second layer. The first-layer Si atoms each have two H neighbors and one dangling bond; the second-layer Si has one H neighbor. This Si_4H_7 cluster is shown in Fig. 2(c).

To study the interaction and the possibility of surface penetration at the open site, a $\text{Si}_{10}\text{H}_{13}$ surface cluster is considered. The Si atoms represent four layers of the surface; three each in the first, second, and third layer, and one in the fourth layer. The fourth-layer atom is in the center of the triangles formed by the three atoms in each of the three other layers. The first-, second-, and fourth-

layer Si atoms each have one embedding H neighbor; the third-layer Si atoms have two hydrogen neighbors. This cluster is shown in Fig. 2(d).

In all adsorption clusters, the distance r with respect to the substrate surface is defined as the distance along a line normal to the surface from the halogen to the plane of the first-layer Si atoms. The equilibrium value of r , r_e , is determined for each cluster by minimizing the total energy of the cluster with respect to variations in r . The binding energy D_e is defined as the cluster energy $E(\text{Si}_n\text{H}_m\text{X})$ for X at r_e less the sum of the total energies of the bare substrate cluster $E(\text{Si}_n\text{H}_m)$ and the isolated halogen atom $E(\text{X})$; $D_e = E(\text{Si}_n\text{H}_m) + E(\text{X}) - E(\text{Si}_n\text{H}_m\text{X})$.

B. Method of calculation

For the calculation of the electronic states of the cluster, we use the SCF HF LCAO method described by Roothaan for both closed-²⁴ and open-²⁵ shell systems. Spin-restricted HF wave functions are calculated using contracted Gaussian-type orbital (CGTO) basis sets of modest size (see Sec. II C). This type of calculation, applied to real molecules, has proved to give results of reasonable accuracy for equilibrium geometries and force constants and to give qualitative guides for relative energies at different points on a potential surface.²⁶ An estimate of the error for the height of the barrier for surface penetration at the open site, a key concern for the reaction process, obtained from the SCF potential curve is given in Sec. IV B. There we discuss our results for H- $\text{Si}(111)$ at the open site²⁷ obtained with a correlated two-configuration multiconfiguration self-consistent-field wave function. Because the clusters treated in the present study are quite large, the energies and wave functions have been generally obtained using the average of configurations formalism²⁸ in order to simplify the calculation. The MOLECULE integral program²⁹ and the ALCHEMY SCF²⁹ program are used for all cluster calculations in this study.

The parameters for vibrations perpendicular to the surface are obtained from the binding-energy curves by using the harmonic approximation. The vibrational energy $\hbar\omega$ is given by

$$\hbar\omega = \hbar(\kappa/m_X)^{1/2},$$

where κ is the curvature of the binding curve at the equilibrium distance r_e and m_X is the mass of the halogen; the mass of the Si substrate is assumed to be infinite. A good rule for molecules is that SCF quadratic force constants are in error by $\sim 15\%$.^{17,26}

In order to simplify the analysis of the results and the interpretation of the bonding of the halogen to the Si substrate, we used the corresponding orbital transformation of Amos and Hall.³⁰ This transformation has been mostly used in the context of the ionization problem.³¹ Here we sketch the approach and point out its useful features for the cluster-model calculations.

Consider two different sets of orthogonal orbitals; for example, let \bar{Q}^1 be a set of q_1 SCF orbitals for a bare substrate cluster and let \bar{Q}^2 be a set of q_2 ($q_2 > q_1$) orbitals for a substrate-atom cluster. The two new sets of corresponding orbitals, \bar{U} and \bar{V} , are unitary transformations of \bar{Q}^1 and \bar{Q}^2 , respectively. In terms of the original orbitals,

the corresponding orbitals are solutions of the eigenvalue equations

$$\begin{aligned} \underline{S} \underline{S}^\dagger \bar{u}_i &= \lambda_i \bar{u}_i, \quad i = 1, \dots, q_1 \\ \underline{S}^\dagger \underline{S} \bar{v}_i &= \lambda_i \bar{v}_i, \quad i = 1, \dots, q_2. \end{aligned} \quad (1)$$

The elements of the $q_1 \times q_2$ overlap matrix \underline{S} are $S_{jk} = (\phi_j^1 | \phi_k^2)$. The corresponding orbitals have the following useful properties:

- (a) $0 \leq \lambda_i = \lambda_i' \leq 1, \quad i = 1, 2, \dots, q_1,$
- (b) $\lambda_i = 0, \quad i = q_1 + 1, \dots, q_2,$
- (c) The overlap $(u_i | v_j) = (\lambda_i \delta_{ij})^{1/2}.$

The corresponding orbital transformation leads to orbitals which have extremal values of overlap between the two sets. The adsorbate-substrate orbitals which have no equivalent in the bare substrate cluster are those for which $\lambda = 0$. The orbitals which have changed most during adsorption have small values of λ ; those which have changed least have large values of λ .

C. Basis sets and symmetry considerations

Because the maximum cluster size $\text{Si}_{10}\text{H}_{15}\text{X}$ considered in the present study is considerably larger than the Si_4H_9 cluster¹⁸ used to study hydrogen adsorption on Si(111), smaller basis sets were used. The choice of an appropriate basis set for the representation of the cluster orbitals is of vital importance for the accuracy of the results.

In order to obtain a compact basis which still gave a

good approximation to the atomic SCF energies, we used a nonsegmented contracted basis set³² for Si and Cl. The set was minimal for the Ne cores ($1s^2 2s^2 2p^6$) and double ζ for the 3s and 3p valence shells. The exponents were taken from the Roos-Siegbahn (10s,6p) optimized sets.³³ Duplication of the primitives to form the nonsegmented constructions led to elementary bases which were effectively 12s 7p for Si and 12s 6p for Cl. These sets were contracted to 4s 3p. The important contraction coefficients of these nonsegmented sets were optimized in calculations on the free atoms. For the 3P state of the Si atom we obtained an energy of -288.701 hartree. The energy with the uncontracted 10s 6p basis is -288.773 hartree³³ and the value of the usual 6s 4p double- ζ contraction is -288.730 (-288.854 is the HF limit³⁴). With the 4s 3p basis for chlorine, the total energy for the 2P ground state of Cl is -459.231 hartree compared to the unconstructed value of -459.358 hartree³³ and -459.287 for the 6s 4p double- ζ basis; the HF limit is -459.482 .³⁴ These basis sets are given in Table I. For F, a segmented contraction to 4s 3p of Van Duijneveldt's 10s 6p primitive set³⁵ was used. The basis set for H is taken from the cluster study on the hydrogen chemisorption on Si(111)¹⁸ (4s contracted to 2s). On the whole, the basis sets used in the present calculations are of, or better than, double- ζ quality for the valence shells; it is unlikely that the results obtained will change significantly if larger basis sets are used. With the use of these basis sets of modest size for the individual atoms, the calculation of the $\text{Si}_{10}\text{H}_{15}\text{X}$ cluster, for example, involves 173 contracted basis functions.

TABLE I. CGTO (4s, 3p) basis sets for Si and Cl derived from the (10s, 6p) primitive set of elementary functions. The elementary-function exponents and normalized contraction coefficients are given.

| Si | | Cl | |
|-------------|--------------|-------------|--------------|
| s exponents | Coefficients | s exponents | Coefficients |
| 19 237.2 | 0.001 597 | 28 656.3 | 0.001 592 |
| 2 885.41 | 0.012 273 | 4 299.00 | 0.012 202 |
| 655.111 | 0.060 987 | 976.335 | 0.060 988 |
| 184.413 | 0.213 651 | 274.415 | 0.213 429 |
| 59.251 6 | 0.457 658 | 89.006 3 | 0.453 700 |
| 20.462 6 | 0.394 168 | 31.237 1 | 0.396 630 |
| 20.462 6 | 0.105 703 | 31.237 1 | 0.117 005 |
| 4.411 16 | -0.446 614 | 7.769 51 | -0.254 303 |
| 1.614 79 | -0.648 726 | 3.079 33 | -0.739 096 |
| 1.614 79 | 0.511 058 | 3.079 33 | 0.523 128 |
| 0.291 392 | -1.226 477 | 0.651 038 | -1.265 808 |
| 0.140 147 | 1.0 | 0.240 298 | 1.0 |
| p exponents | Coefficients | p exponents | Coefficients |
| 95.786 5 | 0.028 313 | 150.436 | 0.028 503 |
| 21.9200 | 0.173 486 | 34.710 1 | 0.177 297 |
| 6.439 88 | 0.472 578 | 10.407 1 | 0.480 085 |
| 1.989 98 | 0.515 089 | 3.373 3 | 0.495 741 |
| 1.989 98 | 0.035 062 | | |
| 0.482 93 | -1.019 203 | 0.748 495 | 1.0 |
| 0.122 84 | 1.0 | 0.207 855 | 1.0 |

The point-group symmetry of all the clusters considered in this work is C_{3v} with the irreducible representations a_1 , e (doubly degenerate), and a_2 . For the integral calculations²⁹ we used symmetry-adapted basis functions which transformed only as a C_s subgroup of C_{3v} . However, in the SCF calculations, we included a further transformation of the Fock operators³⁶ so that they were blocked according to the irreducible representations of C_{3v} . Thus the SCF orbitals belong to irreducible representations of the full symmetry of the clusters.

III. RESULTS AND DISCUSSION FOR THE SUBSTRATE CLUSTERS

A. On-top site clusters: Si_4H_9 and $\text{Si}_{10}\text{H}_{15}$

For this site we are able to compare properties for Si_4H_9 with our basis (see Sec. II C) with those obtained for the same cluster with a larger basis set including d polarization functions.¹⁸ From this comparison we can estimate some of the consequences of using our smaller basis. In Table II we give our SCF total energies for $\text{H}(^2S)$, $\text{Si}(^3P)$, and for several Si_nH_m clusters. The cluster binding energy, given as

$$D = -[E_{\text{tot}}(\text{Si}_m\text{H}_n) - mE_{\text{tot}}(\text{Si}) - nE_{\text{tot}}(\text{H})],$$

is, for Si_4H_9 , 0.91 hartree. A similar value of 1.05 hartree was obtained with the extended basis.¹⁸ In Table III we give representative orbital energies for the substrate clusters. In particular, we give values of the orbital energy for the lowest valence-level orbital, ϵ_l , and the highest closed-shell orbital, ϵ_h . For Si_4H_9 , the range of closed-shell valence-level orbital energies, $\Delta\epsilon = \epsilon_h - \epsilon_l$, obtained with our basis, 0.42, is almost the same as that obtained with the more extended basis of Ref. 18, 0.44 hartree. The small differences between our basis and that of Ref. 18 for the binding energy and the orbital energies strongly support that the binding within the cluster and between cluster and adatom will be described satisfactorily with a minimum core and double- ζ valence-level basis.

The ground state of the Si_4H_9 and $\text{Si}_{10}\text{H}_{15}$ clusters is, as expected, 2A_1 . It has the open-shell configuration a_1^1 where a_1 is the sp_z dangling bond of the top silicon. Qualitative information about the electronic structure of different atoms in the clusters is obtained from a Mulliken population analysis.³⁷ Table IV gives the distribution of the valence ($3s$ and $3p$) electrons on the atoms in different layers of the substrate clusters. The decomposition into s and p contributions indicates redistribution of $\text{Si } 3s$ - and $3p$ -type electrons (compared to the free atom) and hybridization to essentially sp^3 character.¹⁸ The total number of

TABLE II. Electronic ground states and total energies E_{tot} of the hydrogen and silicon atoms and the substrate clusters.

| Cluster | Ground state | E_{tot} (hartree) |
|-------------------------------|-------------------------------|----------------------------|
| H | 2S | -0.4977 |
| Si | 3P | -288.7011 |
| Si_4H_9 | 2A_1 | -1160.1924 |
| $\text{Si}_{10}\text{H}_{15}$ | 2A_1 | -2896.2907 |
| $\text{Si}_{10}\text{H}_{13}$ | $(a^1e^2)_{\text{average}}^a$ | -2894.9690 |
| Si_4H_7 | $(a^1e^2)_{\text{average}}^a$ | -1158.8452 |

^aUse of the average of configurations rather than a particular angular-momentum-coupled state.

valence electrons per Si atom varies from layer to layer. It oscillates about four, the neutral bulk value. For Si_4H_9 , the silicon atom in the first layer has an excess electronic charge; Si in the second layer becomes positive. This dipolar distribution is also reflected in a similar variation of the atomic charge in the first and fourth layers in $\text{Si}_{10}\text{H}_{15}$. From electrostatic arguments, this indicates an attractive force between the two kinds of Si atoms with a tendency to pull the first-layer atoms toward the second layer. This inward relaxation of the first-layer atoms on Si(111) was first proposed by Appelbaum and Hamann³⁸ from band-structure calculations. The variation of the electronic density from layer to layer was also observed by Pandey and Phillips³⁹ in a semiempirical tight-binding calculation for a film of 20 atomic layers in thickness. They calculated both the unrelaxed and relaxed configuration of Si(111). For the relaxed Si(111) surface (0.33-Å contraction), it was found that the effect of relaxation is to reduce the large excess of electrons in the first layer and replace them with a weaker dipolar distribution in the first and second layer. This, in turn, is reflected in a still weaker dipole in the third and fourth layer.

In our calculation, however, the differences in the electronic structures of the first- and second- (and also the third- and fourth-) layer silicon atoms is also due to differences in the environment of these atoms caused by the hydrogen-atom embedding procedure. In the Si_4H_9 cluster, the Si atom of the first layer has a nearest-neighbor environment of three silicon atoms, whereas each of the Si atoms in the second layer is surrounded by one silicon atom and three hydrogen atoms. This must lead to a somewhat different bonding situation. In the $\text{Si}_{10}\text{H}_{15}$ cluster, the Si atoms of the second layer have only two instead of three hydrogen nearest neighbors. They become less positive; 3.74 compared to 3.53 for Si_4H_9 . For the clusters modeling the eclipsed and open sites (see Sec. III B) the situation is reversed. The silicon atoms in the first layer,

TABLE III. Orbital energy range for the silicon valence levels in the bare substrate clusters. The energy of the lowest (highest) doubly occupied valence orbital is ϵ_l (ϵ_h); the range is $\Delta\epsilon = \epsilon_h - \epsilon_l$. The energies of the a_1 - and/or e -symmetry dangling-bond surface orbitals are denoted ϵ_d . All energies are in hartree.

| Cluster | ϵ_l | ϵ_h | $\Delta\epsilon$ | ϵ_d |
|-------------------------------|--------------|--------------|------------------|----------------------------------|
| Si_4H_9 | -0.801 | -0.383 | 0.418 | -0.342 (a_1) |
| $\text{Si}_{10}\text{H}_{15}$ | -0.848 | -0.376 | 0.472 | -0.334 (a_1) |
| $\text{Si}_{10}\text{H}_{13}$ | -0.844 | -0.374 | 0.470 | -0.243 (a_1), -0.244 (e) |
| Si_4H_7 | -0.792 | -0.387 | 0.405 | -0.255 (a_1), -0.247 (e) |

TABLE IV. Distribution of the valence electrons on atoms in different layers of the substrate clusters and its decomposition into s and p contributions from a gross population analysis. The superscript denotes the layer.

| Si ₄ H ₉ | | | | | | | | |
|----------------------------------|------------------|------------------|------------------|------------------|-----------------|-----------------|-----------------|-----------------|
| Contribution | $N(\text{Si})^1$ | $N(\text{Si})^2$ | | | $N(\text{H})^1$ | $N(\text{H})^3$ | | |
| s | 1.46 | 1.23 | | | 1.13 | 1.13 | | |
| p | 2.79 | 2.30 | | | | | | |
| Total | 4.25 | 3.53 | | | 1.13 | 1.13 | | |
| Si ₁₀ H ₁₅ | | | | | | | | |
| Contribution | $N(\text{Si})^1$ | $N(\text{Si})^2$ | $N(\text{Si})^3$ | $N(\text{Si})^4$ | $N(\text{H})^1$ | $N(\text{H})^3$ | $N(\text{H})^4$ | $N(\text{H})^5$ |
| s | 1.45 | 1.28 | 1.35 | 1.27 | 1.13 | 1.08 | 1.04 | 1.08 |
| p | 2.67 | 2.46 | 2.77 | 2.45 | | | | |
| Total | 4.12 | 3.74 | 4.12 | 3.72 | 1.13 | 1.08 | 1.04 | 1.08 |
| Si ₁₀ H ₁₃ | | | | | | | | |
| Contribution | $N(\text{Si})^1$ | $N(\text{Si})^2$ | $N(\text{Si})^3$ | $N(\text{Si})^4$ | $N(\text{H})^1$ | $N(\text{H})^2$ | $N(\text{H})^4$ | $N(\text{H})^5$ |
| s | 1.40 | 1.35 | 1.28 | 1.34 | 1.04 | 1.09 | 1.08 | 1.03 |
| p | 2.40 | 2.77 | 2.44 | 2.77 | | | | |
| Total | 3.80 | 4.12 | 3.72 | 4.11 | 1.04 | 1.09 | 1.08 | 1.03 |
| Si ₄ H ₇ | | | | | | | | |
| Contribution | $N(\text{Si})^1$ | $N(\text{Si})^2$ | | | $N(\text{H})^2$ | $N(\text{H})^4$ | | |
| s | 1.35 | 1.37 | | | 1.12 | 1.04 | | |
| p | 2.33 | 2.83 | | | | | | |
| Total | 3.68 | 4.20 | | | 1.12 | 1.04 | | |

which are surrounded by both Si atoms and embedding H atoms, become positive and the second-layer Si atoms have, in turn, an excess negative charge. Therefore, from the clusters considered in the present study, the variation of electron density in the surface layers cannot be determined exactly. However, the results for the top-layer Si atom in Si₄H₉ and Si₁₀H₁₅, which has the correct environment (only Si nearest neighbors), indicate a dipolar distribution with excess charge in the first layer. The exact amount of charge variation could be reliably calculated only if still larger clusters are considered, e.g., Si₁₃H₇ with seven Si in the first layer and three each in the second and third layers, the silicon atoms of the third layer saturated with hydrogen atoms. For this cluster, atoms of both the first and second layers have only Si atoms as nearest neighbors.

The orbital energy difference $\Delta\epsilon$ between the highest and lowest doubly occupied Si valence orbitals in Si₄H₉ ($\Delta\epsilon=11.4$ eV, see Table III) and Si₁₀H₁₅ ($\Delta\epsilon=12.8$ eV) are close to the energy range of the silicon bulk valence band. From a band-structure calculation, a value of 12.6 eV is obtained.⁴⁰ Synchrotron photoemission measurements⁴¹ give a valence bandwidth of 12.4 ± 0.6 eV. The singly occupied dangling-bond state lies on top of these valence levels; its orbital energy ϵ_d is also given in Table III. This state represents quite well the half-filled dangling-bond surface band which lies in the energy gap between valence and conduction bands of the clean Si(111) surface³⁹ and dominates the electronic properties of the Si semiconductor surface.

B. Open-site cluster: Si₁₀H₁₃

The ground state of the Si₁₀H₁₃ substrate cluster is found to have the open-shell configuration $a_1^1 e^2$ where the

a_1 and e orbitals are different combinations of the essentially sp_z dangling bonds. Its determination is not a trivial matter. Quantum-chemical intuition and group-theoretic analysis usually lead to a correct determination of the ground state for most molecules, especially for those with closed-shell structures. However, for clusters of this size with open-shell structures, differences among the orbital energies of the highest occupied molecular orbitals (MO's) become fairly small. We used a procedure described in detail in earlier cluster calculations.^{17,19} A wave function for the "core cluster" is obtained (only $1s$ orbitals are occupied). Then $2m$ electrons are added in the lowest- m virtual (unoccupied) orbitals of the previous SCF wave function and iterated again to self-consistency. This step is repeated until all electrons are included. In this way the $a_1^1 e^2$ configuration was found to have the lowest total energy, given in Table II. In order to simplify the calculation, the energies and wave functions have been obtained for the average of configurations²⁸ of the $a_1^1 e^2$ open shells rather than for a specific spin and spatial coupling.

The energy range of the doubly occupied Si valence levels (see Table III) is almost identical to the range found for the on-top site substrate cluster. The open-shell dangling bonds a_1 and e show very little splitting. They are shifted upwards by 0.09 hartree compared to the single dangling bond of the head-on site. This shift of about 2 eV is due to the fact that the average of configurations was calculated rather than a specific coupling. We discuss this point in more detail for Si₄H₇ in Sec. IV, where, in addition to the average of configuration are investigated explicitly. The distribution of valence electrons on atoms in different layers, given in Table IV, has been discussed in Sec. III A for the on-top site clusters.

C. Eclipsed-site cluster: Si₄H₇

For the clusters for the threefold sites, both Si₄H₇ and Si₁₀H₁₃, there are different possible occupations for the a_1 and e dangling-bond orbitals. The three possible distributions are, $a_1^1e^2$, e^3 , and a_1^2e . In order to determine the ground-state configuration with reasonable certainty, it is useful to perform separate SCF calculations on the different occupations for a_1 and e . The Si₄H₇ cluster is small enough to permit an investigation of these configurations and also of the effect of specific spin and angular couplings of the open-shell electrons.

Chemical intuition strongly suggests that $a_1^1e^2$ is the ground-state configuration. This is based on considerations of transformation between the delocalized a_1 - and e -symmetry orbitals and localized dangling-bond orbitals on each of the three "surface-layer" Si atoms. The $a_1^1e^2$ distribution transforms, for all but one of the couplings of the open-shell electrons, into singly occupied localized orbitals on each of the three Si atoms. The other distributions transform into linear combinations of configurations involving both singly and doubly occupied localized orbitals. In order to form a configuration with doubly occupied localized dangling-bond orbitals, the energy of removing an electron (ionizing) from one of the surface Si atoms must be recovered. This energy is normally compensated because one of the delocalized symmetry orbitals is deeper and has a lower orbital energy than the other. However, from Table III we see that the a_1 and e orbital energies ϵ_d are nearly the same. Thus $a_1^1e^2$ should contain the ground state. SCF calculations for Si₄H₇ have been performed for $a_1^1e^1(^2E)$, for $e^3(^2E)$, and for the average of configurations²⁸ for $a_1^1e^2$; the results are shown in Table V. It is clear that $a_1^1e^2$ has the lowest total energy and that the ground state has this configuration.

The $a_1^1e^2$ configuration contains four states: one quartet, 4A_2 , and three doublets, 2A_2 , 2E , and 2A_1 . Electron paramagnetic resonance (EPR) of the Si(111) surface has been investigated⁴² and has led Haneman to estimate that there is one unpaired spin per ten surface atoms. In order to investigate the spin couplings of the dangling bonds, SCF calculations were performed for the four states arising from $a_1^1e^2$ and the results are shown in Table V. The total energies show a strong dependence on the spin coupling. The lowest state is the quartet 4A_2 ; it is ~ 30 eV lower in energy than the highest doublet 2A_1 . Thus our simple model for the unreconstructed Si(111) surface suggests that there is essentially one unpaired spin per surface atom, which is quite different from the EPR estimate⁴² of one per ten surface atoms. Of course, larger clusters as

well as variation of the position of the surface atoms in these clusters would have to be considered to substantiate our findings. These effects may ultimately favor a surface with a lower spin density. However, the energy difference between the high-spin and low-spin state is quite large, and there is evidence that relaxation effects are reasonably small on Si(111).²³ This suggests that it may be worthwhile to reexamine the EPR of clean, well-defined Si(111) surfaces.

In Table V the energy range of the doubly occupied Si-type valence levels (ϵ_l , ϵ_h , and $\Delta\epsilon$) and the energy of the dangling-bond states ϵ_d are given for the different couplings of the $a_1^1e^2$ configuration. The explicit spin coupling has its largest effect, of course, on the open-shell a_1 and e levels. In the 4A_2 state their energy is similar and almost identical to the energy of the single dangling-bond state in the Si₄H₉ cluster with one surface silicon atom (see Table III). (For the average of configuration, the orbital energy of these levels is shifted upwards by ~ 2.4 eV.) Thus Si₄H₇ (4A_2), Si₄H₉, and Si₁₀H₁₅ all yield an energy difference of 1.1 eV between the top of the valence-band and the dangling-bond surface state. This result is in excellent agreement with values at the Γ point (zone center) obtained in band-structure-type calculations by Appelbaum and Hamann³⁸ (0.88 eV) and Pandey and Phillipps⁴³ (1.04 eV).

IV. RESULTS AND DISCUSSION FOR THE Si-F CLUSTERS

As discussed in the Introduction, fluorine atoms react spontaneously to form volatile SiF_x products, principally SiF₄.⁶ Thus the adsorption studies discussed below should not be regarded only as studies for chemisorption at different sites but also as model investigations of the possibility for formation of surface species which are likely to be reaction intermediates in the formation and desorption of SiF₄. The combination of results for the interaction of fluorine at the three high-symmetry sites may make it possible to propose a reaction path.

A. On-top site adsorption: (Si₄H₉)F and (Si₁₀H₁₅)F

The lowest configuration for both the (Si₄H₉)F and (Si₁₀H₁₅)F clusters is closed shell. The open-shell (dangling-bond) a_1 orbital of the bare cluster forms a bonding combination with a $2sp_2$ -hybridized fluorine orbital. The interaction energy as a function of F distance from Si is essentially identical for the two clusters; the curve for (Si₄H₉)F is shown in Fig. 3. Here the cluster total energy for a given distance $r_{\text{Si-F}}$ of the fluorine to the

TABLE V. Ground-state configuration, total energy E_{tot} , and the orbital energy range for the silicon valence levels for the Si₄H₇ eclipsed-site cluster. The quantities ϵ_l , ϵ_h , $\Delta\epsilon$, and ϵ_d are defined in Table III. Energies are in hartree.

| State | Configuration | $E_{\text{tot}} + 1158$ | ϵ_l | ϵ_h | $\Delta\epsilon$ | $\epsilon_d(a_1)$ | $\epsilon_d(e)$ |
|----------------------|--------------------------|-------------------------|--------------|--------------|------------------|-------------------|-----------------|
| Average ^a | $a_1^1e^2$ | -0.8452 | -0.792 | -0.387 | 0.405 | -0.255 | -0.247 |
| 2E | e^3 | -0.8222 | -0.792 | -0.386 | 0.406 | | -0.232 |
| 2E | $a_1^2e^1$ | -0.8188 | -0.793 | -0.219 | 0.574 | | -0.261 |
| 4A_2 | $a_1^1(^2A_1)e^2(^3A_2)$ | -0.9760 | -0.790 | -0.385 | 0.405 | -0.343 | -0.348 |
| 2A_2 | $a_1^1(^2A_1)e^2(^3A_2)$ | -0.7994 | -0.793 | -0.385 | 0.408 | -0.353 | -0.286 |
| 2E | $a_1^1(^2A_1)e^2(^1E)$ | -0.8210 | -0.792 | -0.387 | 0.405 | -0.254 | -0.223 |
| 2A_1 | $a_1^1(^2A_1)e^2(^1A_1)$ | -0.8071 | -0.778 | -0.255 | 0.523 | -0.290 | -0.577 |

^aAverage of configurations for the four states arising from $a_1^1e^2$.

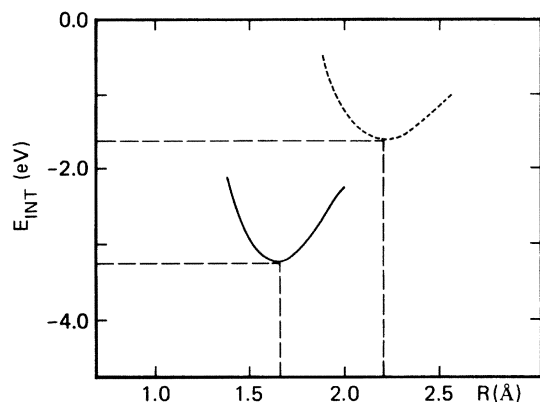


FIG. 3. Interaction-potential curves for $\text{Si}_4\text{H}_9\text{F}$ (solid line) and $\text{Si}_4\text{H}_9\text{Cl}$ (dashed line) as a function of the distance R of the halogen atom from the surface. The interaction-potential curves for the larger cluster $\text{Si}_{10}\text{H}_{15}\text{X}$, $\text{X}=\text{F}, \text{Cl}$, are the same. The zero of the interaction energy E_{int} is the sum of the energies of the substrate cluster and the halogen atom.

central silicon atom is given with respect to the sum of the total energies of the separated F atom and the substrate cluster. The energy at the minimum of the curve defines the fluorine binding energy D_e . The total energy, equilibrium position r_e , and D_e are given in Table VI.

The fluorine equilibrium distance and the binding energy for both clusters are found to be identical. This shows that the adsorbate-substrate binding is localized at the nearest-neighbor environment of the silicon surface. This identity gives strong support that the cluster models and the embedding procedure used in the present study are adequate for the description of the adsorbate-substrate interaction. It also indicates that the results will not be significantly affected if the size of the clusters are increased by adding substrate atoms. The large binding energy of 3.25 eV is comparable to the Si—F bond strength in SiF_4 for which we calculated 3.4 eV with the same basis. The calculated Si—F equilibrium distance (1.68 Å) is only slightly larger than the sum of atomic radii (1.6 Å).⁴⁴

Information about the change in the electronic structure of different atoms in the cluster after adsorption is obtained by comparing the gross atomic valence-electron populations for $(\text{Si}_4\text{H}_9)\text{F}$ and $(\text{Si}_{10}\text{H}_{15})\text{F}$ given in Table VII with the corresponding results for the bare clusters (see Table IV). For both clusters a net charge transfer to the F atom of $-0.58e$ is found. This charge transfer stems exclusively from the first-layer silicon atom; the net charges on the second- (and third- and fourth-) layer Si atoms remain virtually unchanged. In addition, the changes in

the charges of the embedding hydrogen atoms are negligible.

The canonical MO's which are solutions of the HF equations^{24,25} are in general rather delocalized. This usually makes it difficult, especially if the cluster is large, to analyze the results so as to exhibit the properties of bonds. In the $(\text{Si}_{10}\text{H}_{15})\text{F}$ case, for example, the $2sp_z$ orbital, assumed to make a bonding combination with the originally singly occupied Si $3sp_z$ dangling bond, has reasonably large contributions to four of the canonical SCF MO's. The fact that the many-electron wave function is invariant against unitary mixing of the MO's gives considerable flexibility in the choice of occupied orbitals. We therefore use the corresponding orbital transformation to simplify the analysis of the results and the interpretation of the bonding. As discussed in Sec. IIB, the corresponding orbital transformation provides a unique mapping of the orbitals of the bare substrate cluster onto their partners in the cluster which includes an adsorbate. The deviation of the eigenvalues of $\underline{S}\underline{S}^\dagger$ (or $\underline{S}^\dagger\underline{S}$) from unity is a measure of the change of the substrate-corresponding orbitals upon adsorption; see Eq. (1) and related discussion. In Table VIII we present results for the corresponding orbitals with eigenvalues λ less than 1 for $\text{Si}_{10}\text{H}_{15}$ and $\text{Si}_{10}\text{H}_{15}\text{F}$. For these orbitals we give the value of λ and a description of their dominant character.

The three orbitals with eigenvalue zero, the "missing" orbitals in the bare substrate cluster, are, as expected, fluorine orbitals. The smallest eigenvalue (0.408) is that for the Si—F bonding orbital: It is the bare substrate Si $3sp_z$ dangling bond which forms a bonding combination with the F $2sp_z$ orbital. There are only three other Si-type valence orbitals which are slightly perturbed by the adsorption of the fluorine atom. All other substrate orbitals remain unchanged. These results show quantitatively that *only* the Si sp_z dangling bond is strongly affected upon adsorption of the fluorine atom.

The main effect of adsorption at the head-on site in the valence spectrum is the disappearance of the Si dangling-bond surface state at ~ -0.34 hartree (see Table III). The fluorine $2p_x$ and $2p_y$ (e -symmetry) state appears at -0.63 and the Si($3sp_z$)—F($2sp_z$) bond at -0.69 hartree. (These orbital energies are the same for both clusters.) The values are reasonable: The fluorine $2sp_z$ orbital will overlap with the open-shell Si sp^3 hybridized orbital and form a covalent bond having a lower energy (~ 1.7 eV in our calculation) than that of fluorine $2p_{x,y}$ (e -symmetry) orbitals which are not strongly bound to the Si.

The influence of adsorption on the orbital energy ϵ of the nonbonding F $1s$ level will be discussed in Sec. IV D. There we interpret the change of this ϵ as an initial-state shift²⁰ and compare our results for the three F adsorption sites with an XPS study of fluorine interacting with Si.¹⁵

TABLE VI. Electronic ground state, total energy E_{tot} , equilibrium position r_e , and binding-energy D_e of the adsorbing fluorine at the head-on site. The value of r_e gives the distance between the central silicon and the adsorbing fluorine.

| Cluster | Ground state | E_{tot} (hartree) | r_e (bohrs) | D_e (hartree) |
|---|--------------|----------------------------|---------------|-----------------|
| $(\text{Si}_4\text{H}_9)\text{F}$ | 1A_1 | -1259.69 | 3.17 | 0.1196 |
| $(\text{Si}_{10}\text{H}_{15})\text{F}$ | 1A_1 | -2995.79 | 3.17 | 0.1183 |

TABLE VII. Mulliken gross populations for the valence (3s and 3p for Si, 2s and 2p for F, and 1s for H) charge on the distinct atoms of the on-top site F-Si clusters. The Si-F distance, $r = 3.2$ bohrs, is close to r_e . Substrate-atom layers are denoted by a superscript.

| Cluster | Charge | $N(F)$ | $N(Si)^1$ | $N(Si)^2$ | $N(Si)^3$ | $N(Si)^4$ | $N(H)^1$ | $N(H)^3$ | $N(H)^4$ | $N(H)^5$ |
|--------------------|----------|--------|-----------|-----------|-----------|-----------|----------|----------|----------|----------|
| $(Si_4H_9)F$ | <i>s</i> | 2.01 | 1.36 | 1.23 | | | 1.11 | 1.13 | | |
| | <i>p</i> | 5.57 | 2.43 | 2.30 | | | | | | |
| | Charge | -0.58 | +0.21 | +0.47 | | | -0.11 | -0.13 | | |
| $(Si_{10}H_{15})F$ | <i>s</i> | 2.01 | 1.34 | 1.28 | 1.35 | 1.27 | 1.07 | 1.08 | 1.03 | 1.08 |
| | <i>p</i> | 5.57 | 2.32 | 2.46 | 2.78 | 2.45 | | | | |
| | Charge | -0.58 | +0.34 | +0.26 | -0.13 | +0.28 | -0.07 | -0.08 | -0.03 | -0.08 |

B. Open-site adsorption: $(Si_{10}H_{13})F$

With the use of the average of configuration formalism, several open-shell configurations were investigated to determine the one with the lowest energy. In order to understand the bonding at this site, it is helpful to recall that the F-atom ground-state p^5 configuration may, in the C_{3v} symmetry of the cluster, be either $e^4a_1^1$ with a hole in p_z or $e^3a_1^2$ with a hole in p_{xy} . The bare cluster $Si_{10}H_{13}$ ground-state configuration is $a_1^1e^2$ where both orbitals are dangling bonds. This a_1 -substrate orbital forms, in $(Si_{10}H_{13})F$, a largely ionic bond with the a_1^1 open shell of the $e^4a_1^1$ configuration of F. The lowest-energy configuration of $(Si_{10}H_{13})F$ has only an e^2 dangling-bond open shell. The interaction-potential curve, as a function of F distance from the surface, is shown in Fig. 4.

There is a minimum of -0.56 eV for F 1.3 \AA above the surface. For this well the Si-F distance is 2.6 \AA , which is somewhat larger than the sum of the Si and F ionic radii,⁴⁵ 2.4 \AA . There is a second minimum of -0.49 eV at -1.4 \AA below the surface. This well is between the second and third layers of Si atoms, and the barrier for surface penetration is ~ 1 eV (see Fig. 4). We believe that the error of the SCF approximation is to make the barrier height somewhat too large. In a closely related study of the penetration of H at this Si threefold site²⁷ we found that the inclusion of key electron correlation effects lowered the barrier by 0.9 eV with respect to the SCF value. Thus we expect that for an unrelaxed and unreconstructed Si(111) surface, the barrier for F surface penetra-

tion would be less than ~ 0.5 eV. At thermal energies, F atoms could easily penetrate this barrier and be bound in the inner potential well.

The gross atomic population analysis for $(Si_{10}H_{13})F$, for F in the equilibrium positions both above and below the surface, is presented in Table IX. Comparison of Table IX with the results for the bare substrate cluster in Table IV show that for the outer well only the first-layer Si atoms are significantly affected; they transfer charge to the adsorbing F. This is quite similar to the result found for the on-top site. However, the ionicity of the F atom, -0.70 , is somewhat larger than for the on-top site, -0.58 . When fluorine penetrates into the surface and stabilizes between the second and third layer a net charge transfer of $-0.47e$ to F is found. In this case the first-layer silicon atoms are, as expected, much less affected, whereas the Si atoms of the second, third, and fourth layer all lose some charge. This suggests that the change in the interaction between the Si atoms adjacent to the F and their nearest Si neighbors could result in relaxation and reconstruction in such a way as to accommodate the F atom. This reconstruction could lower the penetration barrier and increase the depth of the inner well; hence, it would lead to an even greater probability for F surface penetration.

The variation of the F ionicity is also given in Table IX as its distance along the surface normal is varied. It suggests that charge transfer from Si to F and the resulting Coulomb attraction may play an important role in the interaction. (We consider only the results for F near the surface since the SCF wave function dissociates incorrectly²⁷;

TABLE VIII. Corresponding orbitals for $Si_{10}H_{15}$ and $(Si_{10}H_{15})F$ which have eigenvalues λ less than 1. The dominant character of these orbitals is described. The results are for F 3.2 bohrs above the surface.

| λ | C_{3v} Point-group symmetry | Character | |
|-----------|-------------------------------|--|---|
| | | $(Si_{10}H_{15})F$ | $Si_{10}H_{15}$ |
| 0 | a_1 | F(1s) | |
| 0 | a_1 | F(2s and $2p_z$) | |
| 0 | <i>e</i> | F(2p) | |
| 0.4076 | a_1 | Bonding combination first layer Si($3sp_2$) and F($2sp_2$) | Dangling-bond first layer Si($3sp_2$) |
| 0.9953 | <i>e</i> | Si valence 3s and 3p | Si valence 3s and 3p |
| 0.9986 | a_1 | | |
| 0.9999 | a_1 | | |

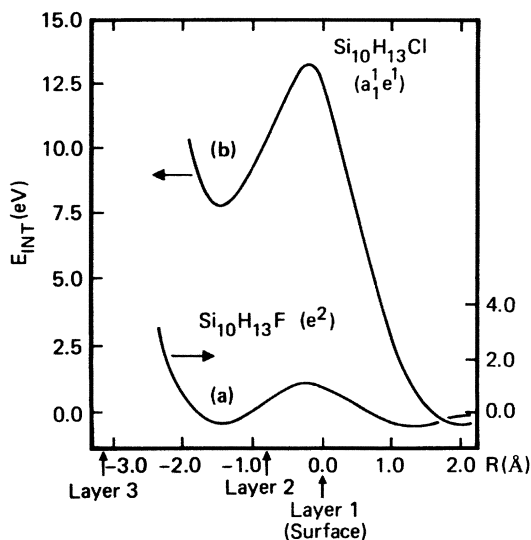


FIG. 4. Interaction-potential curves for $\text{Si}_{10}\text{H}_{13}\text{F}$ (a) and $\text{Si}_{10}\text{H}_{13}\text{Cl}$ (b) as a function of the distance R of the halogen atom from the surface. The zero of the interaction energy E_{int} is the sum of the energies of the substrate cluster and the halogen atom. The positions of the layers of the Si surface are marked. The right-hand scale for E_{int} is for (a) and the left-hand scale is for (b).

at large separation, it goes to $\text{Si}_{10}\text{H}_{13}^+$ and F^- .) As F approaches closer to the surface than the first minimum, $r = +2.6$ bohrs, the F ionicity decreases as the F-Si interaction becomes repulsive. At the barrier maximum, $r = -0.4$ bohrs, the ionicity -0.22 is minimum. Then charge transfer increases and the interaction again becomes attractive. A relative maximum of charge $0.47e$ is transferred at the inner well, $r = -2.8$ bohrs.

A very similar view of the bonding is given by the corresponding orbital analysis. The corresponding orbitals between $\text{Si}_{10}\text{H}_{13}$ and $(\text{Si}_{10}\text{H}_{13})\text{F}$ with eigenvalues λ less than 1 are given in Table X. The three orbitals with $\lambda=0$

are the fluorine $1s(a_1)$, $2p(e)$, and a $2sp(a_1)$ combination. From a population analysis, the character of the $2sp$ orbital is $0.2(2s) + 0.8(2p_z)$ where the plus sign indicates that it is hybridized away from the Si. The orbital with the smallest nonzero $\lambda=0.026$ is essentially $0.8(2s) - 0.2(2p_z)$. The small value indicates that the bonding is highly ionic. The bare cluster $3sp_z$ dangling bond changes into the $\text{F}2sp_z$ hybrid in $(\text{Si}_{10}\text{H}_{13})\text{F}$. This is quite different from the on-top site situation where the smallest $\lambda=0.408$ and the dangling bond maps into a covalent Si-F covalent bond. The next smallest $\lambda=0.993$ is the surface dangling bond of e symmetry. The large value of λ shows that it is only slightly affected by F adsorption. The remaining orbitals given in Table X are essentially Si $3sp$ cluster valence orbitals; they have large λ 's and are almost unperturbed by the F adsorption.

Examination of the cluster SCF orbital energies show that the dominantly fluorine $2p_{xy}$ state appears at -0.720 hartree, only slightly modified from the $2p$ value of -0.731 hartree for the free atom, whereas the eigenvalues for vectors with $\text{F}2p_z$ contributions lie mostly around -0.450 hartree, above the $2p_{xy}$ orbital energy. This is again consistent with chemical intuition for this more ionic site. The difference in the F core-level orbital energies between adsorption at the "covalent" on-top and "ionic" open sites will be considered in Sec. IV D.

C. Eclipsed-site adsorption: $(\text{Si}_4\text{H}_7)\text{F}$

To complete the study of the interaction of fluorine with the Si(111) surface we discuss briefly the results for the eclipsed site. Owing to the presence of the second-layer Si atom which is only 0.78 \AA below the surface, the bonding situation is different from the open site. The lowest-energy configuration for $(\text{Si}_4\text{H}_7)\text{F}$ has an $a_1^1 e^1$ dangling-bond open-shell occupation. The e^3 shell of $\text{F}2p^5$ in the $a_1^2 e^3$ configuration has formed a bonding combination with the e^2 shell of the bare Si_4H_7 cluster

TABLE IX. Mulliken gross populations for the valence charge on the distinct atoms of the $(\text{Si}_{10}\text{H}_{13})\text{F}$ cluster for F at the outer and inner wells. The gross atomic charges are given for F as a function of F to Si surface distance, $r(\text{Si-F})$. Substrate-atom layers are denoted by a superscript.

| $r(\text{Si-F})$ (bohr) | Charge | $N(\text{F})$ | $N(\text{Si})^1$ | $N(\text{Si})^2$ | $N(\text{Si})^3$ | $N(\text{Si})^4$ | $N(\text{H})^1$ | $N(\text{H})^2$ | $N(\text{H})^4$ | $N(\text{H})^5$ | |
|----------------------------|----------|---------------|------------------|------------------|------------------|------------------|-------------------|-----------------|-----------------|-------------------|-------|
| 2.6 | <i>s</i> | 1.97 | 1.39 | 1.35 | 1.28 | 1.34 | 1.03 | 1.08 | 1.08 | 1.03 | |
| Outer well | <i>p</i> | 5.73 | 2.20 | 2.77 | 2.45 | 2.77 | | | | | |
| | Charge | -0.70 | +0.41 | -0.12 | +0.27 | -0.11 | -0.03 | -0.08 | -0.08 | -0.03 | |
| -2.8 | <i>s</i> | 1.91 | 1.43 | 1.37 | 1.28 | 1.34 | 1.06 | 1.09 | 1.09 | 1.06 | |
| Inner well | <i>p</i> | 5.56 | 2.28 | 2.71 | 2.39 | 2.70 | | | | | |
| | Charge | -0.47 | +0.29 | -0.08 | +0.33 | -0.05 | -0.06 | -0.09 | -0.09 | -0.06 | |
| $r(\text{Si-F})$ (bohr) | 4.0 | 3.0 | 2.6 ^a | 1.8 | 1.0 | 0.2 | -0.4 ^b | -1.2 | -2.0 | -2.8 ^a | -3.6 |
| F charge | -0.84 | -0.74 | -0.70 | -0.59 | -0.45 | -0.29 | -0.22 | -0.28 | -0.40 | -0.47 | -0.42 |

^aPosition of minima of the wells.

^bPosition of the maximum of the surface penetration barrier.

TABLE X. Corresponding orbitals for the $(\text{Si}_{10}\text{H}_{13})\text{F}$ and $\text{Si}_{10}\text{H}_{13}$ clusters which have eigenvalues λ less than 1. The results are for the outer well with F 2.6 bohrs above the surface. The dominant orbital character is described.

| λ | C_{3v} Point-group symmetry | $(\text{Si}_{10}\text{H}_{13})\text{F}$ | Character | $\text{Si}_{10}\text{H}_{13}$ |
|-----------|-------------------------------|---|-----------|--|
| 0 | a_1 | F(1s) | | |
| 0 | a_1 | F[0.2(2s)+0.8(2p _z)] | | |
| 0 | e | F(2p) | | |
| 0.0259 | a_1 | F[0.8(2s)-0.2(2p _z)] | | Si(3s _{p_z}) dangling bond |
| 0.9933 | e | Si dangling bond | | Si dangling bond |
| 0.9956 | a_1 | Si valence 3s and 3p | | Si valence 3s and 3p |
| 0.9992 | e | | | |
| 0.9998 | a_1 | | | |
| 0.9998 | e | | | |
| 0.9999 | e | | | |

(open-shell configuration $a_1^1e^2$), leading to a e^4e^1 occupation for these 5e-symmetry electrons. The interaction-potential curve is shown in Fig. 5. There is a shallow well with $D_e=0.49$ eV at $R=1.72$ Å above the surface. The increase in the position of the minimum by 0.4 Å over that for the open site is due to the presence of the second-layer Si atom. The influence of this atom and the resulting Coulomb repulsion is clearly seen in the steep ascent of the potential curve after the minimum. Though it is possible that a fluorine atom stabilizes above this site, it is the most unlikely site to play a role in the interaction of F with Si(111). It yields a low binding energy and there is no possibility for penetration of the surface.

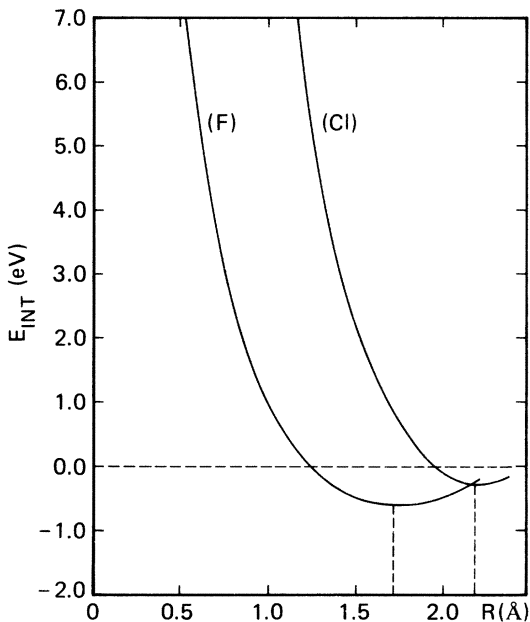


FIG. 5. Interaction-potential curves for $\text{Si}_4\text{H}_7\text{F}$ (F) and $\text{Si}_4\text{H}_7\text{Cl}$ (Cl) as a function of the distance R of the halogen atom from the surface.

D. Site-dependent variation of core-level binding energies

An XPS study of a Si crystal exposed to XeF_2 showed a complex F(1s) structure.¹⁵ A rather broad peak with a full width at half maximum (FWHM) of 4.3 eV is observed for the dissociative XeF_2 adsorption. This broad band suggests that the adsorbed F atoms are in different chemical environments or adsorption sites. The band clearly contains two maxima at 685.5 and 687.2 eV. When the silicon is heated to 550°C, the F 1s peak becomes narrower, FWHM of 2.5 eV, and shows a single maximum at 685.5 eV. The Si 2s and Si 2p spectra after exposure to XeF_2 are reasonably similar to those obtained for a clean surface: The Si 2s and Si 2p peaks are at ~ 151 and ~ 100 eV, respectively.

For the interpretation of these spectra we consider the cluster core-level orbital energies ϵ_i . In Table XI we present values of $-\epsilon_i$ for the F 1s and for the Si 2s and Si 2p orbitals of the first- and second-layer atoms of the $(\text{Si}_{10}\text{H}_{15})\text{F}$ on-top and $(\text{Si}_{10}\text{H}_{13})\text{F}$ open-site clusters. For Si we give the average for the closely spaced energies of the different 2s or 2p orbitals that arise for the atoms of a given layer. [The results for the two on-top site clusters $(\text{Si}_4\text{H}_9)\text{F}$ and $(\text{Si}_{10}\text{H}_{15})\text{F}$ are essentially identical.] These orbital energies are taken as Koopmans's-theorem (KT) unrelaxed ionization potentials (IP's). The F 1s IP at the on-top site is 714.7 eV. The IP for F above the surface at the open site is lower by 3.8 eV. For F which has penetrated the surface and is at the open-site inner well, the IP is 1.4 eV lower than the on-top site IP. Thus the F 1s IP varies as much as 3.8 eV depending on adsorption geometry. The KT IP's are so much larger than the observed IP's because of the final-state relaxation energy; for the free F atom⁴⁶ this is 20 eV. However, the variation of the orbital energy at different adsorption sites should be a reasonably accurate reflection of the variation of the relaxed IP's. Even though there are large changes for the F 1s ϵ 's, 3.8 eV, the changes among the Si 2s and Si 2p ϵ 's are relatively small, ~ 1 eV.

A comparison of the KT IP's with the XPS results suggests that the F is adsorbed initially at sites both above and below the Si surface. When the Si is heated the higher-binding-energy portion of the F 1s band, corresponding to F above the surface, becomes much less intense, and the low-binding-energy portion, corresponding to F below the surface, remains.

TABLE XI. Koopman's-theorem IP's for F(1s), Si(2s), and Si(2p) for (Si₁₀H₁₅)F on top and (Si₁₀H₁₃)F open-site cluster calculations. The Si IP's are averages over the orbitals for a given layer of atoms in the cluster. A superscript denotes the Si layer: Si¹, first layer; Si², second. For the open site, results are given for the outer well (above) and the inner well (below). The IP's are in eV.

| Core level | (Si ₁₀ H ₁₅)F | (Si ₁₀ H ₁₃) Open site | |
|----------------------|--------------------------------------|---|-------|
| | On-top Site | Above | Below |
| F(1s) | 714.7 | 710.9 | 713.4 |
| Si ¹ (2s) | 168.7 | 167.9 | 167.6 |
| Si ² (2s) | 167.5 | 167.3 | 167.3 |
| Si ¹ (2p) | 117.5 | 116.7 | 116.4 |
| Si ² (2p) | 116.3 | 116.1 | 116.1 |

V. RESULTS AND DISCUSSION FOR THE Si-Cl CLUSTERS

The study of the interaction of Cl with a Si surface is parallel to that discussed above for F and analogous cluster models are used. The binding energy and the equilibrium distance above the surface are summarized in Table XII for all three sites considered. The on-top site has, by far, the largest D_e and is clearly the most stable. In Secs. VA–VC we present the results for the on-top, open, and eclipsed sites, respectively. In Sec. VD we present an analysis of the surface vibrational frequencies and compare the behavior found for the different sites.

A. On-top site adsorption: (Si₄H₉)Cl and (Si₁₀H₁₅)Cl

The lowest-energy configuration for both clusters is, as for F, a closed-shell ¹A₁ state. The Cl 3p_z hybridizes and forms a bonding combination with the bare cluster open-shell a₁ orbital. The interaction-energy curve $E_{\text{int}}(r)$ near r_e is shown in Fig. 3. As for F, r_e and D_e for both clusters are found to be the same indicating localization of the chlorine-silicon binding to the nearest neighbor on the silicon surface and demonstrating quantitatively the absence of cluster size effects. The chlorine binding energy of 1.63 eV found for Cl chemisorbed on top of a surface silicon atom is higher than the calculated Si–Cl bond strength in SiCl₄ for which we obtained 1.08 eV with the same basis. The calculated Si-Cl equilibrium distance (2.24 Å) is somewhat larger than the sum of covalent (atomic) radii (2.16 Å) and larger by about 10% than the Si–Cl bond length in SiCl₄ (2.04 Å). These bond distances were used in previous band-structure calculations^{14,47} of Cl-Si(111) at the on-top site.

The valence charge on the cluster atoms and its decomposition into *s* and *p* contributions is given in Table XIII. In both clusters there is a transfer of 0.39 electrons from the Si atoms to Cl. Comparing with the results for the bare substrate clusters, Table IV, we see that this charge transfer comes almost entirely from the first-layer silicon atom.

We again used the corresponding orbital transformation to examine the change in the cluster orbitals. As in the fluorine case, there is only one eigenvalue (except for the chlorine 1s, 2s, 2p, 3s, and 3p_{xy} orbitals which have zero eigenvalues) which deviates significantly from one (0.578), indicating that only one bare cluster orbital is strongly affected upon chemisorption. The corresponding orbital is, in the substrate cluster, the Si 3s_z dangling bond. In the Cl-Si cluster the Si dangling orbital has formed a bond of a₁ type with the Cl 3s-3p_z orbital. Only three other Si-type valence levels are slightly influenced by the chlorine adsorption. Their corresponding eigenvalues are 0.9989 (*e*), 0.9994, and 0.9999 (both a₁).

The calculated cluster D_e 's conclusively show that Cl adsorbs at the on-top site. In the absence of this sort of reliable adsorbate binding-energy calculations it is difficult to estimate the adsorption site. The large electronegativity difference between Cl and Si favors an ionic threefold, open or eclipsed site. On the other hand, forming a strong Si–Cl covalent bond favors the onefold on-top site. However, these should lead to different photoemission spectra (PES). Analysis of the PES has been used to support adsorption at the on-top site.^{7,10–13,47} Thus it is interesting to compare our calculated valence spectrum (KT's orbital energies) with experimental PES results.

The ultraviolet photoemission spectroscopy (UPS) spectrum of Cl-Si(111) shows a chlorine-induced peak somewhat above the middle of the Si valence spectrum with a lower-energy shoulder.¹² Another significant change in the UPS spectrum caused by Cl adsorption is the reduction in the emission intensity near the top of the valence band. Employing *s*- and *p*-polarized photons to study the symmetry character of the spectral features, the shoulder is identified to have σp_z character, whereas the main peak is due to π_{px,y} orbitals.⁴⁷

We have constructed a histogram by counting the orbitals with orbital energies within 0.05 hartree (1.36 eV). This histogram is shown in Fig. 6 for both the (Si₁₀H₁₅)Cl, dotted lines, and for the bare Si₁₀H₁₅, solid lines, clusters. The main effect of chlorine adsorption is the disappearance of the Si dangling-bond surface state at –0.34 hartree which has formed a bonding combination with the Cl 3p_z orbital and is shifted downwards to –0.48 hartree. This is in agreement with the observed reduction in the emission intensity at the top of the valence band. The or-

TABLE XII. Electronic ground state, total energy E_{tot} , equilibrium position r_e , and binding-energy D_e , of the adsorbing chlorine at the three high-symmetry positions.

| Cluster | Ground state | E_{tot} (hartree) | r_e (bohr) | D_e (hartree) |
|---------------------------------------|--|----------------------------|--------------|-----------------|
| (Si ₄ H ₉)Cl | ¹ A ₁ | –1619.4850 | 4.22 | 0.061 |
| (Si ₁₀ H ₁₅)Cl | ¹ A ₁ | –3355.5820 | 4.23 | 0.060 |
| (Si ₁₀ H ₁₃)Cl | (a ₁ ¹ e ¹) _{average} | –3354.2162 | 3.67 | 0.016 |
| (Si ₄ H ₇)Cl | (a ₁ ¹ e ¹) _{average} | –1618.0840 | 4.17 | 0.008 |

TABLE XIII. Mulliken gross populations for the valence ($3s$ and $3p$ for Cl and Si and $1s$ for H) charge on the distinct atoms of the clusters for Cl-Si(111) at on-top and open sites. The populations are for a Cl to surface distance r close to the equilibrium value. Substrate-atom layers are denoted by a superscript.

| Cluster | Charge | $N(\text{Cl})$ | $N(\text{Si})^1$ | $N(\text{Si})^2$ | $N(\text{Si})^3$ | $N(\text{Si})^4$ | $N(\text{H})^1$ | $N(\text{H})^a$ | $N(\text{H})^4$ | $N(\text{H})^5$ |
|---------------------------------------|--------|----------------|------------------|------------------|------------------|------------------|-----------------|-----------------|-----------------|-----------------|
| (Si ₄ H ₆)Cl | s | 2.00 | 1.39 | 1.23 | | | 1.11 | 1.13 | | |
| $r = 4.2$ bohrs | p | 5.39 | 2.64 | 2.28 | | | | | | |
| On top | Charge | -0.39 | -0.03 | +0.48 | | | -0.11 | -0.13 | | |
| (Si ₁₀ H ₁₅)Cl | s | 2.00 | 1.38 | 1.28 | 1.35 | 1.27 | 1.07 | 1.08 | 1.03 | 1.08 |
| $r = 4.2$ bohrs | p | 5.39 | 2.53 | 2.44 | 2.78 | 2.45 | | | | |
| On top | Charge | -0.39 | +0.09 | +0.28 | -0.13 | +0.28 | -0.07 | -0.08 | -0.03 | -0.08 |
| (Si ₁₀ H ₁₃)Cl | s | 1.98 | 1.38 | 1.35 | 1.28 | 1.34 | 1.04 | 1.08 | 1.08 | 1.03 |
| $r = 3.6$ bohrs | p | 5.47 | 2.30 | 2.74 | 2.47 | 2.77 | | | | |
| Open | Charge | -0.45 | +0.32 | -0.09 | +0.25 | -0.11 | -0.04 | -0.08 | -0.08 | -0.03 |

^aSecond-layer H for (Si₄H₆)Cl and (Si₁₀H₁₃)Cl and third-layer H for (Si₁₀H₁₃)Cl.

bitals with mainly Cl $3p_{xy}$ character lie above the σp_z orbital. Our results for the valence spectrum are, therefore, in agreement with the observed PES spectra and the generally accepted interpretation.

From the binding curves the parameters for chlorine vibrations perpendicular to the surface can be obtained, see Sec. II B. The results are given in Table XIV. The values for the curvature κ and the vibrational energies are almost identical for (Si₄H₆)Cl and (Si₁₀H₁₅)Cl, indicating again that the adsorbate-substrate bonding is strongly localized.

B. Open-site adsorption: (Si₁₀H₁₃)Cl

We investigated several configurations, using the average of configurations, in order to find the one with the lowest energy. The lowest-energy configuration for (Si₁₀H₁₃)Cl has $a_1 e^1$ dangling-bond open shells, in contrast to the e^2 open shell found for (Si₁₀H₁₃)F. Here the open e^3 shell ($3p_{xy}$) of Cl in an $a_1^2 e^3 (3p^5)$ configuration has formed a bonding combination with a surface Si electron of e symmetry. The difference in bonding between these two cases arises because Cl is larger than F. For example, for F, $\langle r \rangle_{2p} = 0.57$ Å, whereas for Cl, $\langle r \rangle_{3p} = 0.97$ Å. [This result is different from the interpretation usually employed that, in the threefold-coordinated geometry, the open a_1 shell ($3p_z$) of Cl is completed by Si electrons, and, therefore, expected to be less strongly bound than the $p_{x,y}$ orbitals.] The results for r_e and D_e are given in Table XII and the interaction potential curve is shown in Fig. 4. The situation is quite different from the fluorine adsorption.

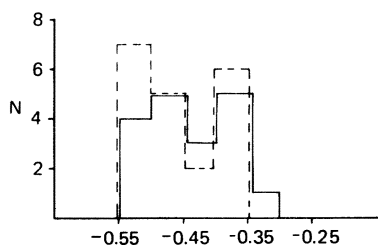


FIG. 6. Number of levels N in an energy range of 0.05 a.u. in the upper part of the valence region before (solid line) and after chlorine chemisorption (dashed line) at the on-top site.

As for F, there is an outer well with a minimum at 1.9 Å and a depth of 0.46 eV. This equilibrium position corresponds to a Si-Cl distance of 2.92 Å which is slightly larger than the sum of ionic radii, 2.81 Å.⁴⁶ However, the barrier for penetration of the surface (~ 13 eV) is much larger than for F (~ 1 eV)—a consequence of the larger size of Cl. Even taking into account that the SCF calculation overestimates, somewhat, the height of the barrier and that Si reconstruction may lower the barrier, Cl atoms will be unable, with any reasonable probability, to penetrate such a large barrier. Thus although the reaction to form, e.g., SiCl₄ from Cl₂ is exothermic by 6.8 eV,⁸ the reaction cannot proceed because Cl cannot penetrate the surface to form a suitable SiCl_x reaction intermediate. This is consistent with the observation that Cl atoms do not spontaneously etch Si under normal conditions but that some form of energetic radiation incident on the surface will make the reaction proceed.⁴⁸

The valence-electron populations for the cluster are given in Table XIII for Cl very near r_e of the outer well. The gross charge on Cl indicates a -0.45 ionicity which is only slightly larger than the -0.39 ionicity found for the on-top site. Comparison with the bare substrate-cluster populations, Table IV, shows that $\frac{4}{5}$ of the charge transferred to Cl comes from the top-layer Si atoms. Although the charge on Cl is somewhat less than that of F adsorbed at the open site (-0.70), it is still substantial. The Coulomb attraction between the anionic Cl and the positively charged surface-layer Si atoms acts to reduce the barrier for surface penetration. However, there is a large Pauli repulsion from the overlap of the Cl and Si charge distributions due to the large size of Cl. This term is dominant and gives rise to the large, 13-eV penetration barrier. Therefore, suitable candidates for Si surface penetration, and hence spontaneous etching reactions, are atoms with a large electron affinity (which will lead to large Coulombic attraction) but also with small enough size to minimize the Pauli repulsion.

The larger size of Cl also leads to larger overlap populations between it and the surface Si atoms than were found for F. This overlap makes it difficult to assign consistent values for the ionicity of Cl as a function of its distance from the Si surface. This prevents us from making an analysis of the relation between the adsorbate ionicity and

TABLE XIV. Parameters for chlorine vibrations perpendicular to the Si surface. Here κ is the curvature of the interaction-potential curve at equilibrium r_e . The vibrational energy ω_e is determined in the harmonic approximation with the substrate mass assumed infinite. Relative values of the effective spring constants k_n are also given.

| Site | Cluster | κ (hartree/ a_0^2) | ω_e (cm $^{-1}$; meV) | k_n |
|----------|---------------------------|------------------------------|-------------------------------|-------|
| On top | (Si $_4$ H $_9$)Cl | 0.1425 | 326;40.4 | |
| On top | (Si $_{10}$ H $_{15}$)Cl | 0.1400 | 323;40.1 | 1 |
| Open | (Si $_{10}$ H $_{13}$)Cl | 0.0483 | 190;23.5 | 0.27 |
| Eclipsed | (Si $_4$ H $_7$)Cl | 0.0577 | 208;25.8 | 0.28 |

the attractive or repulsive character of the interaction potential as we did in the case of F; see Sec. IV C.

The vibrational parameters are given in Table XIV. The vibrational energy of Cl at the on-top site is larger by a factor of 1.7 than it is at the open site. This difference will be discussed in more detail in Sec. V D.

C. Eclipsed-site adsorption: (Si $_4$ H $_7$)Cl

Here again the lowest-energy configuration has $a_1 e^1$ dangling-bond open shells; the same as found for the open site. The interaction-potential curve is shown in Fig. 5; r_e and D_e are given in Table XII and ω_e in Table XIV. We find an outer well with a minimum at 2.20 Å and a depth of 0.22 eV. The equilibrium distance from the surface is larger by 0.3 Å than that found for the open site. The steep ascent of the potential after the minimum strongly shows the presence of the second-layer Si atom and the resulting Pauli repulsion. The order of binding energies ($D_{\text{eclipsed}} = 0.22$ eV < $D_{\text{open}} = 0.43$ eV < $D_{\text{head on}} = 1.63$ eV) implies that the eclipsed site is the least probable site for adsorption of Cl.

D. Site dependence of the vibrational energies of Cl

The frequencies of chlorine vibrations perpendicular to the surface, given in Table XIV, are clearly dependent on the site coordination of the adsorbed Cl. It is largest for the on-top site (onefold) and smallest (threefold) site. The difference between the open and the eclipsed site (also threefold) is rather small. In order to separate the effects of different numbers and different strengths of bonds, we consider a simple spring model used by Froitzheim *et al.* to interpret vibrational excitations of oxygen⁴⁹ and hydrogen⁵⁰ adsorbed on a tungsten surface. It is assumed that the adsorbate vibration is determined by a superposition of springs connecting the adsorbate with the nearest substrate surface atoms. Then

$$\omega_e(n) = C \cos \alpha_n (nk_n)^{1/2}, \quad (2)$$

where n is the number of nearest neighbors for the site, α is the angle between the bond and the surface normal, k_n is the force constant of the springs, and C is a constant which depends on the mass of the adsorbate. Froitzheim *et al.*^{49,50} made the assumption that nk_n is constant although there is no obvious reason why this should be so. It was found that this sum rule holds for H on Be(0001).¹⁷ For O on Li(100),¹⁹ the model was not applicable at all.

Applied to Cl on Si(111), we obtained the relative values of k_n given in Table XIV. Clearly, the effective bond

force constants are quite different for the onefold and threefold sites, but about equal for the two threefold sites. The relation $nk_n = 1$ does not hold; it is rather $3k_3 \sim 0.8$.

The absolute values for the vibrational energies of 40 and 24 meV for the on-top and open site, respectively, are rather small. The error^{17,26,51} for the computed force constants should be $\leq 15\%$. The difference of ~ 20 meV between these sites may be resolvable with EELS; see, for example, Ref. 50. EELS experiments for Cl-Si(111) might give additional information to verify the on-top adsorption site; they would also serve as a further test of the utility of cluster-model calculations.

VI. CONCLUSION

The present HF SCF calculations on the different Si-F and Si-Cl adsorption clusters as well as on the respective substrate clusters give insight into the nature of interaction and chemisorption of fluorine and chlorine on the Si(111) surface. Except for one non-self-consistent slab calculation,¹⁴ no prior F-Si(111) calculations exist; for Cl, these are the first cluster calculations and provide new information regarding bond energy and distance and vibrational frequency not obtained from previous band-structure studies.^{7,10-13,47} Clearly, the substrate clusters used here are too small to reproduce all details of the surface electronic structure. However, we have shown that the calculated valence bandwidth and the position of surface dangling-bond states are in satisfactory agreement with experiment. Furthermore, the properties of the adsorbate-substrate interaction are well converged with respect to cluster size. This convergence demonstrates the strong localization of the halogen-silicon surface bonding.

The interactions of the adsorbing fluorine and chlorine with the silicon surface differ significantly among the three high-symmetry sites. The on-top site is energetically most favorable for both halogens. Here the fluorine stabilizes at $r_e = 1.68$ Å above the first silicon layer with an SCF binding energy of $D_e = 3.25$ eV. This distance is only slightly larger than the sum of the covalent radii of Si and F. The binding energy is comparable to our calculated SCF Si-F bond strength in SiF $_4$, 3.4 eV. For Cl, $r_e = 2.24$ Å, which is somewhat larger than the sum of the covalent radii and $D_e = 1.63$ eV. This binding energy is larger than the calculated SCF Si-Cl bond strength SiCl $_4$, 1.08 eV.

The interaction at the open site is very different between F and Cl. For fluorine, there is a well above the surface with $D_e = 0.56$ eV and $r_e = 1.3$ Å. This corresponds to a Si-F distance of 2.6 Å, which is somewhat larger than the

sum of ionic radii, 2.4 Å. In addition, there is a second well with about the same depth, 0.5 eV, at 1.4 Å below the surface, between the second and third layer. The height of the barrier for penetration is ~1 eV. For Cl there is an outer well with a minimum at 1.9 Å and a depth of 0.46 eV. The corresponding Si-Cl distance of 2.9 Å is larger than the sum of ionic radii, 2.81 Å. The barrier to penetrate the surface, however, is much larger, ~13 eV. This is a consequence of the larger size of Cl. The variation of charge transfer to fluorine along the surface normal indicates that ionicity and resulting Coulomb attraction play an important role in the penetration process at the open site.

The eclipsed site has the smallest binding energy. For F, $r_e = 1.72$ Å and $D_e = 0.49$ eV; for Cl, $r_e = 2.20$ Å and $D_e = 0.22$ eV.

Improvement in the basis sets used in the SCF calculations could lead to changes in the calculated D_e of ~10%. Correlation effects, not considered in the SCF approximation, may lead to significant changes in the D_e . However, these effects are not likely to change our computed order of D_e for the different sites:

$$D_e(\text{eclipsed}) \leq D_e(\text{open}) < D_e(\text{on top}) .$$

Thus the onefold on-top site is clearly the most stable site for the adsorption of Cl-Si(111). In addition, the computed valence spectrum for Cl at this site is in agreement with experimental PES spectra. We predict that the vibrational frequencies for Cl motion normal to the surface differ by ~20 meV between the on-top and the threefold open and eclipsed sites. EELS measurements of these frequencies could provide a further demonstration that adsorption is at the on-top site.

The assumption and errors of the calculation are likely to lead to too high a barrier and too shallow an inner minimum in the potential curve for the interaction at the open site. First, surface relaxation and reconstruction, ignored in the cluster model of the Si surface, would prob-

ably be such as to accommodate the fluorine atom and hence lower the barrier and increase the depth of the inner well. Second, the error which the SCF model gives for the penetration barrier due to the neglect of correlation effects can be estimated. In our study of the interaction of H at the open site of Si(111),²⁷ we found that using a simple correlated multiconfiguration SCF wave function led to an 0.9 eV or 30% decrease in the barrier height compared to the SCF value. However, the errors due to our neglect of surface reconstruction and of correlation are much smaller than the over 10-eV difference between the calculated barriers for penetration of F and Cl. The computed F core-level IP's compared to the observed XPS spectra¹⁵ provide strong evidence that F atoms do indeed penetrate the surface. The fact that F atoms penetrate the surface is entirely consistent with the observed spontaneous reactivity to form SiF₄ as the major reaction product.⁶ Assume that F atoms have penetrated the lattice at three adjacent open sites, forming an SiF₃ complex. It will then be easy to form SiF₄ by adsorption of another fluorine directly over the central site. Because of the strong internal bonds in the very stable SiF₄ it is likely to be only weakly bound to the rest of the surface and should easily desorb into the gas phase. Etching of the Si substrate and the formation of volatile SiF₄ occurs. The fact that chlorine atoms cannot penetrate the surface is consistent with the observation that Cl atoms chemisorb and do not easily react spontaneously.

The corresponding orbital transformation has been applied for the first time to surface cluster-model calculations. The mapping of bare substrate orbitals onto their partners in the adsorbate state provides a useful measure of the changes that take place upon adsorption.

Altogether, the present study shows that the MO cluster method can be used to obtain a detailed and, we believe, reasonably accurate description of various aspects of the adsorption of halogens on a silicon surface. The results explain the observed different reactivity of fluorine and chlorine and provide a model for understanding reaction mechanisms relevant in plasma etching.

*On leave from the Institute for Theoretical Chemistry, University of Erlangen-Nürnberg, D-8520 Erlangen, West Germany.

¹See, e.g., J. Appelbaum and D. R. Hamann, *Rev. Mod. Phys.* **48**, 479 (1976), and references therein.

²H. F. Winters, J. W. Coburn, and E. Kay, *J. Appl. Phys.* **48**, 4973 (1977); J. W. Coburn and H. F. Winters, *J. Vac. Sci. Technol.* **16**, 391 (1979).

³J. W. Coburn and H. F. Winters, *J. Appl. Phys.* **50**, 3189 (1979).

⁴H. F. Winters, *J. Appl. Phys.* **49**, 5165 (1978).

⁵H. F. Winters and J. W. Coburn, *Appl. Phys. Lett.* **34**, 70 (1979).

⁶(a) Y. Y. Tu, T. J. Chuang, and H. F. Winters, *Phys. Rev. B* **23**, 823 (1981); (b) H. F. Winters and F. Houle, *J. Appl. Phys.* **54**, 1218 (1983).

⁷P. K. Larson, N. V. Smith, M. Schlüter, H. H. Farrell, K. M. Ha, and M. L. Cohen, *Phys. Rev. B* **17**, 2612 (1978).

⁸*JANAF Thermochemical Tables*, Natl. Stand. Ref. Data Ser., Natl. Bur. Stand. (U.S.) Circ. No. 37 (U.S. GPO, Washington,

D.C., 1971).

⁹V. I. Pepkin, Y. A. Lebedev, and A. Y. Apin, *Zh. Fiz. Khim.* **43**, 1564 (1963).

¹⁰M. Schlüter and M. L. Cohen, *Phys. Rev. B* **17**, 716 (1978).

¹¹J. E. Rowe, G. Margaritondo, and S. B. Christman, *Phys. Rev. B* **16**, 1581 (1977).

¹²K. C. Pandey, T. Sakurai, and H. D. Hagstrum, *Phys. Rev. B* **16**, 3648 (1977).

¹³K. Mednick and C. C. Lin, *Phys. Rev. B* **17**, 4807 (1978).

¹⁴M. Chen and I. P. Batra, *J. Vac. Sci. Technol.* **16**, 570 (1979).

¹⁵T. J. Chuang, *J. Appl. Phys.* **51**, 2614 (1980).

¹⁶For a review see S. R. Morrison, *The Chemical Physics of Surfaces* (Plenum, New York, 1977), p. 169; or the introduction of Ref. 19.

¹⁷(a) C. W. Bauschlicher, Jr., P. S. Bagus, and H. F. Schaefer III, *IBM J. Res. Dev.* **22**, 213 (1978); (b) P. S. Bagus, H. F. Schaeffer, and C. W. Bauschlicher, *J. Chem. Phys.* **78**, 1390 (1983).

¹⁸K. Hermann and P. S. Bagus, *Phys. Rev. B* **20**, 1603 (1979).

¹⁹K. Hermann and P. S. Bagus, *Phys. Rev. B* **17**, 4072 (1978).

- ²⁰P. S. Bagus, K. Hermann, and M. Seel, *J. Vac. Sci. Technol.* **18**, 435 (1981), and references therein.
- ²¹See, e.g., K. C. Pandey, *IBM J. Res. Dev.* **22**, 250 (1978).
- ²²R. W. G. Wyckoff, *Crystal Structures* (Interscience, New York, 1964), Vol. II.
- ²³J. A. Appelbaum and D. R. Hamann, *Phys. Rev. Lett.* **31**, 106 (1973).
- ²⁴C. C. J. Roothaan, *Rev. Mod. Phys.* **23**, 69 (1951).
- ²⁵C. C. J. Roothaan, *Rev. Mod. Phys.* **32**, 179 (1960); C. C. J. Roothaan and P. S. Bagus, *Methods Comput. Phys.* **2**, 47 (1963).
- ²⁶H. F. Schaefer, III, *The Electronic Structure of Atoms and Molecules* (Addison-Wesley, Reading, 1972).
- ²⁷M. Seel and P. S. Bagus, *Phys. Rev. B* **23**, 5464 (1981).
- ²⁸J. C. Slater, *Quantum Theory of Atomic Structure* (McGraw-Hill, New York, 1960), Vol. I.
- ²⁹MOLECULE was written by J. Almlöf of the University of Uppsala, Sweden. The ALCHEMY SCF program was written by P. S. Bagus and B. Liu of the IBM Research Laboratory, San Jose. The interfacing of these programs was performed by U. Wahlgren, University of Uppsala, and P. S. Bagus.
- ³⁰A. T. Amos and G. G. Hall, *Proc. R. Soc. London Ser. A* **263**, 483 (1961).
- ³¹R. L. Martin and E. R. Davidson, *Phys. Rev. A* **16**, 1341 (1977).
- ³²T. H. Dunning, Jr. and P. J. Hay, *Modern Theoretical Chemistry*, edited by H. F. Schaefer (Plenum, New York, 1977), Vol. 3.
- ³³B. Roos and P. Siegbahn, *Theor. Chim. Acta* **17**, 209 (1970).
- ³⁴E. Clementi, *Atomic Energy Tables*, Supplement to *IBM J. Res. Dev.* **9**, 1 (1965).
- ³⁵F. B. Van Duijneveldt, Report No. IBM RJ945 (unpublished).
- ³⁶P. S. Bagus and U. I. Wahlgren, *Comp. Chem.* **1**, 95 (1976).
- ³⁷R. S. Mulliken, *J. Chem. Phys.* **23**, 1833 (1955); **23**, 1841 (1955); **23**, 2338 (1955); **23**, 2343 (1955).
- ³⁸J. A. Appelbaum and D. R. Hamann, *Phys. Rev. Lett.* **31**, 106 (1973).
- ³⁹K. C. Pandey and J. C. Phillips, *Phys. Rev. B* **13**, 750 (1976).
- ⁴⁰M. L. Cohen and T. K. Bergstresser, *Phys. Rev.* **141**, 789 (1966).
- ⁴¹W. D. Grobman and D. E. Eastman, *Phys. Rev. Lett.* **29**, 1508 (1972).
- ⁴²D. Haneman, *Phys. Rev.* **170**, 705 (1968).
- ⁴³K. C. Pandey and J. C. Philipps, *Phys. Rev. Lett.* **32**, 1433 (1974).
- ⁴⁴J. C. Slater, *Symmetry and Energy Bands in Crystals* (Dover, New York, 1972).
- ⁴⁵The radii of F^- and Cl^- are given by L. Pauling, *Nature of Chemical Bonds* (Cornell University Press, New York, 1945). The Si^+ radius is given in Ref. 47.
- ⁴⁶J. Q. Broughton and P. S. Bagus (unpublished).
- ⁴⁷M. Schlüter, J. E. Rowe, G. Margaritondo, J. M. Ho, and M. L. Cohen, *Phys. Rev. Lett.* **37**, 1632 (1976).
- ⁴⁸U. Gerlach-Meyer, J. W. Coburn, and E. Kay, *Surf. Sci.* **103**, 177 (1981).
- ⁴⁹H. Froitzheim, H. Ibach, and S. Lehwald, *Phys. Rev. B* **14**, 1362 (1976).
- ⁵⁰H. Froitzheim, H. Ibach, and S. Lehwald, *Phys. Rev. Lett.* **36**, 1549 (1976).
- ⁵¹P. S. Bagus, I. P. Batra, C. W. Bauschlicher, and R. Broer, *J. Electron Spectrosc. Relat. Phenom.* **29**, 225 (1983).